

# DEUTSCHES ELEKTRONEN-SYNCHROTRON **DESY**

DESY 78/25  
May 1978



RECENT RESULTS FROM THE PLUTO AND DASP DETECTORS AT DORIS

by

J. Simon

NOTKESTRASSE 85 · 2 HAMBURG 52

To be sure that your preprints are promptly included in the  
HIGH ENERGY PHYSICS INDEX ,  
send them to the following address ( if possible by air mail ) :

DESY  
Bibliothek  
Notkestrasse 85  
2 Hamburg 52  
Germany

RECENT RESULTS FROM THE PLUTO AND DASP DETECTORS AT DORIS <sup>+</sup>)

presented by

U. Timm

Deutsches Elektronen-Synchrotron, DESY, Hamburg, F.R.G.

## ABSTRACT

Decays of the heavy lepton  $\tau$  have now been observed in  $e^+e^-$  - collisions at the energy of the  $\psi'$ -resonance, which results in an improved mass determination  $M_\tau = 1.807 \pm 0.020$  GeV. For the  $\tau$ -lifetime a new upper limit of  $\tau_\tau \leq 3.5 \cdot 10^{-12}$  sec. is given. The evidence for the decay  $\tau \rightarrow \nu\pi\rho$  has been strengthened, and the  $\pi\rho$ -system is found to be in an S-wave state with  $J^P = 1^+$ , proving the axial vector component in the leptonic coupling of the  $\tau$  to hadrons. The branching ratio is given with  $BR(\tau^- \rightarrow \nu\pi^-\rho^0) = 0.050 \pm 0.015$ . The total hadronic cross section agrees within errors with the quark sum rule including QCD-corrections. The production and decay distributions of the decay  $J/\psi \rightarrow f^0\gamma$  have been measured and found to agree well with a QCD calculation based on the exchange of two gluons.

## INTRODUCTION

The results reported here have been obtained by the two detectors PLUTO and DASP at the  $e^+e^-$  -storage ring DORIS in the period following the latest Lepton-Photon-Conference held in Hamburg, August 1977. The institutions and physicists involved in these experiments are listed in references 1,2. My talk covers the following subjects :

- mass of the  $\tau$
- lifetime of the  $\tau$
- the decay  $\tau \rightarrow \nu\pi\rho$
- the total  $e^+e^-$  hadronic cross section
- angular distribution of the decay  $J/\psi \rightarrow f^0\gamma$ .

## MASS OF THE TAU

3

The first publication concerning the observation of a new heavy lepton quoted a mass between 1.6 and 2.0 GeV. Since that time the mass value of the  $\tau$  has narrowed down by measurements from PLUTO <sup>4</sup>,  $M_\tau = 1.79 - 1.92$  GeV, and, more recently by the LBL-SLAC lead glass wall detector <sup>5</sup>  $M_\tau = 1.80 - 1.85$  GeV, where the  $\tau$  has

<sup>+</sup>)Talk given at the 3rd International Conference at Vanderbilt University on New Results in High Energy Physics, Nashville, Tennessee, USA, 6-8 March 1978.

been observed at the  $\psi'$  resonance. The accuracy in the mass determination increases the more as we approach the production threshold. There is now an observation of  $\tau$ -decays at the energy of the  $\psi'$ , below the charm threshold.

This experiment has been carried out by the DASP-collaboration<sup>6</sup> with the double arm spectrometer shown in fig. 1. The two spectrometer arms shown cover  $0.072 \text{ str.}$ . A particle emerging from the  $e^+e^-$  - interaction region passes three proportional wire chambers in front of the magnet, six spark chambers behind of it, time of flight- and shower-counters, steel absorbers and range counters.

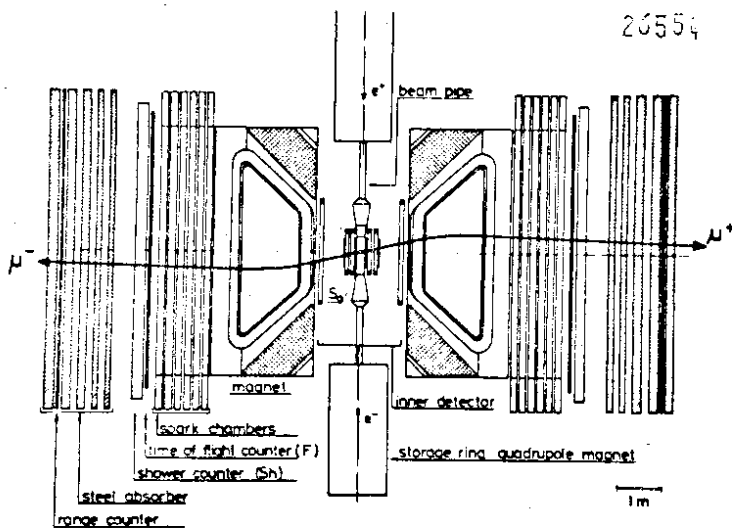


Fig. 1. Plan view of the double arm spectrometer DASP at DORIS.

with four layers of sandwiches, consisting of scintillators, lead and proportional tube chambers, and a lead scintillator shower counter. This part is shown in fig. 2. It covers  $0.70 \times 4\pi \text{ str.}$ . Two Cerenkov counters have been inserted to improve the electron identification in the outer arms in order to detect electrons from  $\tau^-$  (and charm-) decays. The resulting suppression of hadrons achieved is given by the probability of misidentification for hadrons with  $P_{h \rightarrow e} = 4 \cdot 10^{-4}$ .

with four layers of sandwiches, consisting of scintillators, lead and proportional tube chambers, and a lead scintillator shower counter. This part is shown in fig. 2. It covers  $0.70 \times 4\pi \text{ str.}$ . Two Cerenkov counters have been inserted to improve the electron identification in the outer arms in order to detect

The detector is triggered on a single track in one of the outer arms, requiring a momentum  $p \geq 0.4$  GeV/c at  $\sqrt{s} = 3.684$  GeV, and  $p \geq 0.1$  GeV/c at other energies,  $3.1 \leq \sqrt{s} \leq 5.2$  GeV. The events are selected according to the following signatures :

$$\begin{aligned} e^+ e^- &\rightarrow e^\pm + lpr + n \cdot \gamma & (1) \\ e^+ e^- &\rightarrow \mu^\pm + lpr + n \cdot \gamma \\ e^+ e^- &\rightarrow e^\pm \mu^\pm + \text{nothing.} \end{aligned}$$

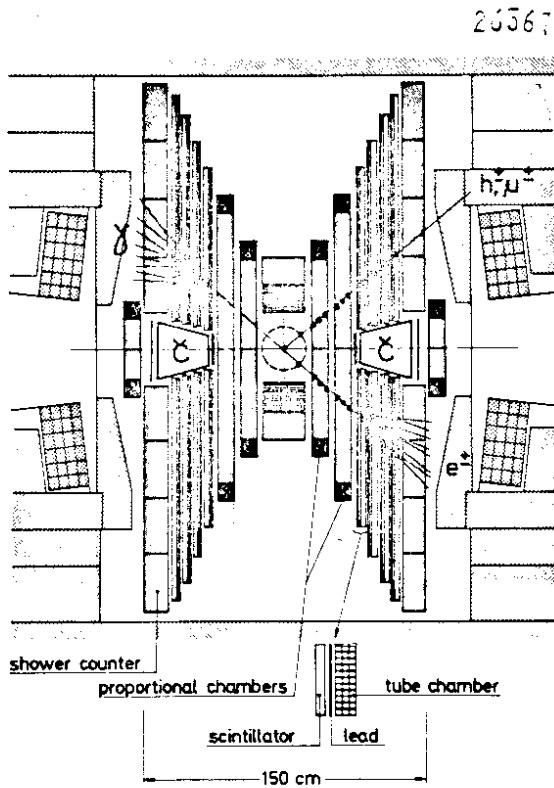


Fig. 2. View in beam direction of the inner DASP-detector.

I restrict myself here to the data sample (1) at  $\sqrt{s} = 3.864$  GeV, where  $1400 \text{ nb}^{-1}$  have been collected and 17 events been found. The momentum distribution of these events is shown in fig. 3. The cluster around 1.5 GeV/c is explained by the cascade decay  $\psi' \rightarrow J/\psi + X \rightarrow e^+ e^- X$ , where X are photons, and one electron is misidentified in the inner detector as hadron ( $P_{e \rightarrow h} = 2 \cdot 10^{-2}$ ). The 9 events in the second cluster are compared by the hypothesis that these events come from the decay  $\tau \rightarrow \nu e \nu$  with  $M = 1.80$  GeV

and a massless neutrino (solid line). Being on the  $\psi'$  resonance, the production of pairs is enhanced over normal QED by a factor of 2.3. The effective luminosity was derived from the number of elastic muon pairs observed in the outer detector. The hypothesis clearly is compatible with the observed event distribution. The background to these events is estimated as follows :

$ee\mu\mu$	0.6 evts.
beam-gas	< 0.1 evts.
$h \rightarrow e$	0.84 evts.
Dalitz pairs	0.2 evts.
total	< 1.7 evts.

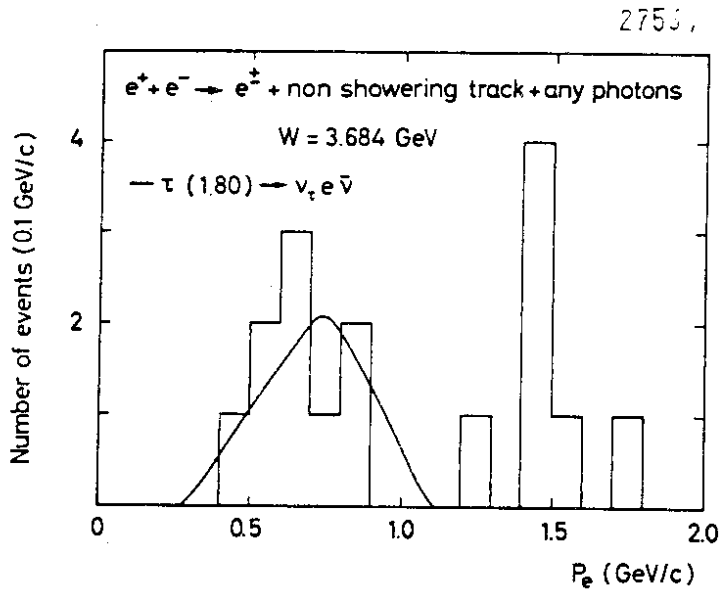
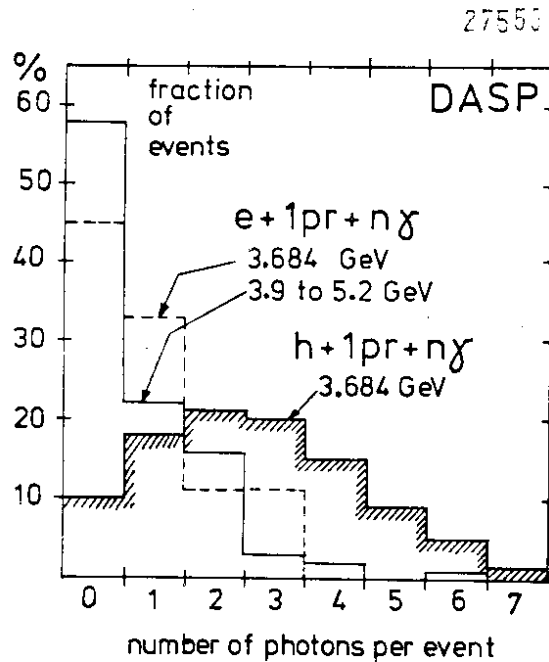


Fig. 3.  
 Electron momentum  
 distribution ob-  
 served at  
 $\sqrt{s} = 3.864 \text{ GeV}$ ,  
 data sample (1)

Fig. 4.  
 Photon multiplicity dis-  
 tributions for event class  
 (1) compared to the equi-  
 valent hadron class at  
 $\sqrt{s} = 3.864 \text{ GeV}$ .



The conclusion is that a significant signal is observed in the momentum spectrum, which is compatible with the decay  $\tau \rightarrow \nu e \bar{\nu}$ .

A further proof that these events come from  $\tau$ -decays is demonstrated by the accompanying photon multiplicities shown in fig. 4. While the distribution for the electron class (1) observed at the  $\psi'$  agrees well with the same class observed all the way up to 5.2 GeV, it drastically disagrees with the equivalent hadron class at the  $\psi'$ . The conclusion is that the electron events seen at the energy of the  $\psi'$  are in fact coming from the decay  $\tau \rightarrow \nu e \gamma$ .

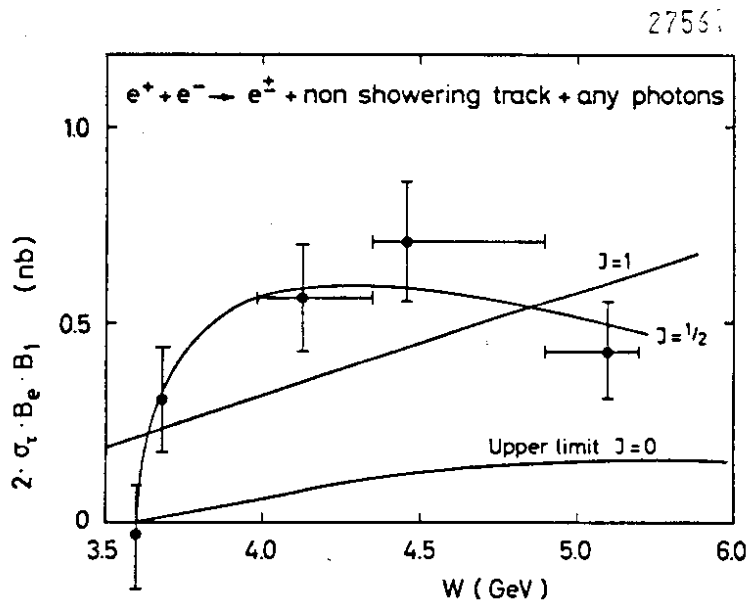


Fig. 5. Integrated inclusive cross section for event class (1) as function of  $\sqrt{s}$ .

cross section is plotted in fig. 5, where the solid line, marked  $J = 1/2$ , is a fit of the data to the threshold function of  $\tau\bar{\tau}$ -production  $2\sigma_{\tau\tau} = \sigma_{\mu\mu} \beta(3 - \beta^2)$ , with  $\beta = (1 - (M_\tau/E_{\text{beam}})^2)^{1/2}$ . The fit yields a mass value of  $M_\tau = 1.807 \pm 0.020$  GeV for the  $\tau$ .

This observation of  $\tau$  below the charm threshold for the first time separates unambiguously the phenomena of charm and heavy lepton.

The mass determination then includes the total amount of data for the event class (1) taken up to  $\sqrt{s} = 5.2$  GeV. The integrated inclusive

#### LIFETIME OF THE TAU

From measurements with the PLUTO detector, a lifetime limit was given of  $\tau_\tau \leq 1 \cdot 10^{-11}$  sec at the time of the Hamburg-Conference<sup>7</sup>. The lifetime expected on the basis of a sequential heavy

lepton is given by

$$\tau_o = BR(\mu) \cdot \tau_\mu (M_\mu/M_\tau)^5 = 2.7 \cdot 10^{-13} \text{ sec} \quad (2)$$

with  $BR(\mu) = 0.18$ ,  $\tau_\mu$ ,  $M_\mu$  the lifetime and mass of the muon, and  $M_\tau = 1.807 \text{ GeV}$ . The analysis has been refined resulting in an improvement of the upper limit quoted earlier.

For the lifetime determination events of the two prong class (3) with one identified muon and no photons are studied :

$$e^+e^- \rightarrow \mu^\pm + \text{lpr} + \text{missing mass} \quad (3)$$

These events have been discussed in a previous publication<sup>4</sup> where it was shown to originate from  $\tau$ -decays. The data have been taken between  $\sqrt{s} = 3.9$  and  $5.0 \text{ GeV}$ , with a total integrated luminosity of  $5600 \text{ nb}^{-1}$ . We found 131 events of type (3) with a momentum  $p_\mu \geq 1 \text{ GeV}/c$ , 53 of which are used for the lifetime analysis. They have an average center of mass energy  $\sqrt{s} = 4.5 \text{ GeV}$ .

The detector is shown in fig. 6. It is a  $4\pi$ -spectrometer of compact design, due to its superconductive coil, which produces a uniform magnetic field of 2 T. The space inside the coil, 1.4 m diameter and 1.05 m length, contains 14 cylindrical proportional chambers, interleaved with two lead converters of thickness 0.44 and

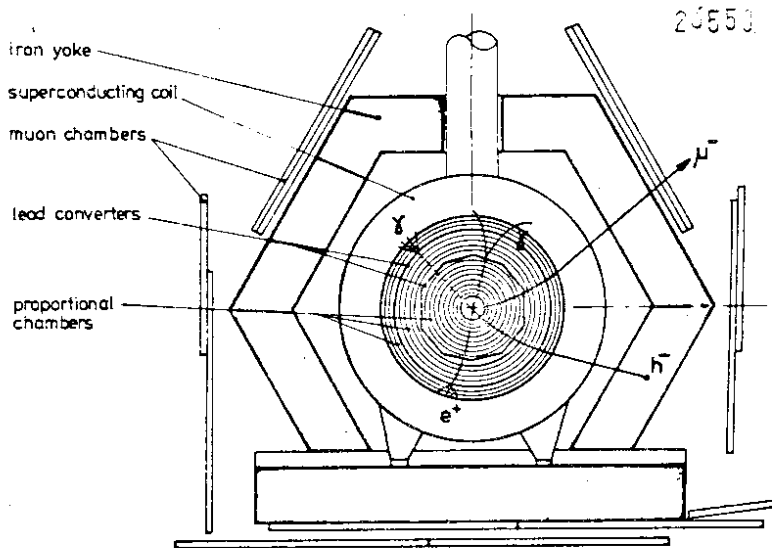


Fig. 6. The detector PLUTO, view in beam direction.



1.72 radiation lengths respectively. The converters allow the identification of photons and electrons through pair production, Bremsstrahlung or showerdevelopment, which are detected in the subsequent chambers. The surrounding iron yoke acts as muon filter. Hadrons are stopped by nuclear reactions and the penetrating muons,  $p_{\mu} \geq 1 \text{ GeV}/c$ , are detected in proportional tube chambers covering the outer surface. Due to the iron thickness ( $\sim 70 \text{ cm}$  average) and the short decay length for  $\pi \rightarrow \mu\nu$ ,  $K \rightarrow \mu\nu$  the misidentification of muons is low :  $P_{h \rightarrow \mu} = 2.8 \cdot 10^{-2}$ .

To get an idea of the experimental approach to the problem, the decay length expected from the lifetime (2) is given at

$$\sqrt{s} = 2E_{\text{beam}} = 4.5 \text{ GeV}$$

$$d = c\tau_0\beta\gamma = c\tau_0 \left( \left( \frac{E_{\text{beam}}}{M_{\tau}} \right)^2 - 1 \right)^{1/2} = 0.067 \text{ mm.}$$

In view of the fact that the beam size at DORIS is three times as large,  $\sigma_x = \sigma_y = 0.2 \text{ mm}$ , and that the origin is reconstructed from tracks with a precision  $\sigma_r = 0.5 \text{ mm}$ , it becomes evident that the experiment yields only an upper limit at the energies available at present.

A quantity which is sensitive to the decay length  $d$  is the distance  $r_{\text{min}}$  of the extrapolated track from the origin, as indicated in fig. 7. The resulting Gaussian distribution of  $r_{\text{min}}$  from

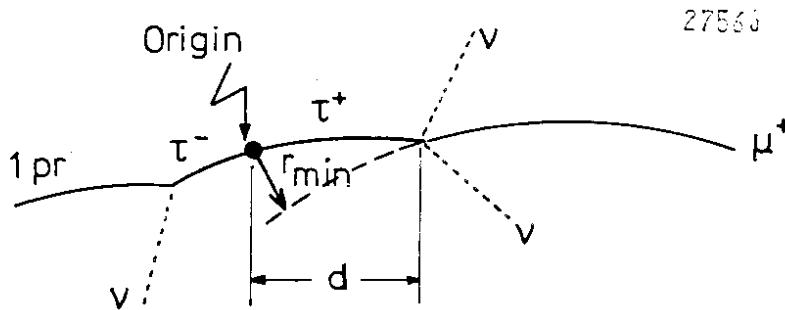


Fig. 7. Decay schematic for  $e^+e^- \rightarrow \tau^+\tau^- \rightarrow \nu\mu\nu + \nu + \text{lpr}$ .

a set of events is characterized by  $\sigma(r_{\text{min}}, d)$ . As explained above, the experiment yields this quantity only at zero decay length,

whereas the dependence on  $d$  has to be studied by a Monte Carlo program, which generates the final state (3) according to the production and decay of a  $\tau$ -pair (see fig. 7). The program simulates the tracks and reanalyses them to obtain the distribution of  $r_{\min}$  by varying the decay length.

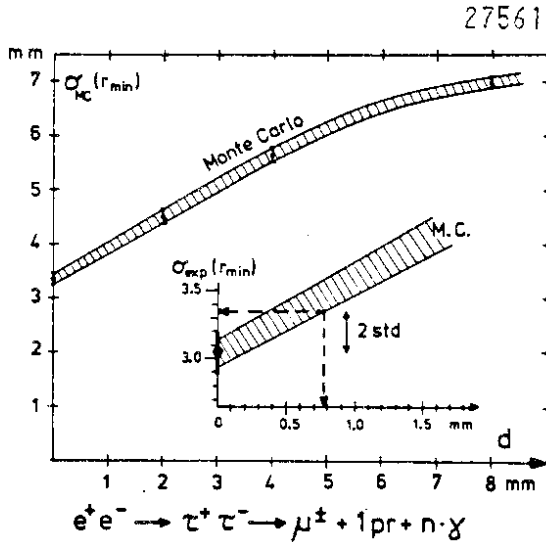


Fig. 8. Monte-Carlo result  $\sigma_{MC}(r_{\min})$  as function of decay length  $d$  of the  $\tau$ , compared to the experimental value  $\sigma_{\exp}(r_{\min}, 0)$ .

The Monte Carlo results are given as function of the decay length in fig. 8. The width of the errors is indicated, and repeated in the insert, scaled to the statistically best experimental value at  $d = 0$  of  $\sigma_{\exp}(r_{\min}, 0) = 3.05 \pm 0.15$  mm deduced from the data sample (3). If its 2 standard deviations error is projected on to the lower error bound from Monte Carlo, a maximum decay length  $d \leq 0.8$  mm is obtained, corresponding to an upper limit

$$\tau_\tau \leq 3.5 \cdot 10^{-12} \text{ sec; } 95 \% \text{ CL.} \quad (4)$$

The new lifetime limit, which can also be expressed as a ratio,  $\tau_\tau/\tau_0 \leq 13$ , has the following bearing on the nature of the

From extensive studies of the pure muon and pure hadron samples, and a comparison between them and the  $\tau$ -sample as defined by equ. (3), we made sure that at zero decay length the value obtained from the Monte Carlo simulation,  $\sigma_{MC}(r_{\min}, 0)$ , is well understood. This investigation becomes necessary since  $\sigma_{\exp}(r_{\min}, 0)$  not only depends on the momenta, but also is somewhat sensitive to the difference in multiple scattering of muons and hadrons.

The Monte Carlo results are given as function of the decay length in fig. 8. The

$\tau$ -neutrino :

(1) If the  $\nu_\tau$  is identical with the old muon neutrino  $\nu_{\mu L}$ , the  $\tau$  can be produced in neutrino beams via the reaction

$\nu_{\mu L} + N \rightarrow \tau^- + \dots e^- + \dots$ , where the observation of soft electrons indicates the  $\tau$ -decay. Both FNAL and CERN bubble chamber groups<sup>8,9</sup>, have looked for this process and quoted lower limits  $\tau_\tau(\nu_\mu)/\tau_0 > 40$  and 15 respectively. Thus the lefthanded muon neutrino is ruled out as possible  $\tau$ -neutrino.

(2) In models<sup>10</sup>, where the  $\tau$ -neutrino is of heavy mass,  $M_{\nu_\tau} > M_\tau$ , the decay can only proceed via mixing to the old neutrinos,

$\nu_\tau + \epsilon_e \nu_e + \epsilon_\mu \nu_\mu$ , where the limits on the mixing parameters,  $\epsilon_e, \epsilon_\mu < 0.1$ , are derived from nuclear reactions. The lower limit on the lifetime ratio for this model is then  $\tau/\tau_0 = (\epsilon_e^2 + \epsilon_\mu^2)^{-1} > 50$ , which exceeds the PLUTO limit and excludes a heavy mass neutrino.

#### THE DECAY $\tau \rightarrow \nu\pi\rho$

This decay was first reported on the Hamburg Conference<sup>7</sup> and has been published<sup>11</sup>. Since that time the statistics was increased by extending the  $e\pi\pi\pi$  sample and by including events of the type  $\mu\pi\pi\pi$ .

The experiment has been carried out with the PLUTO detector by investigating the final state

$$e^+e^- \rightarrow \ell\pi\pi\pi + \text{missing mass} \quad (5)$$

where  $\ell = e$  or  $\mu$ , the charge of the four particles is balanced and no photon is detected. It has to be shown, that the majority of the event sample (5) originates from the production and decay of  $\tau$ -pairs in the reaction

$$e^+e^- \rightarrow \tau^+\tau^- \rightarrow \ell\nu\nu + \pi\pi\pi\nu, \ell = e, \mu \quad (6)$$

27559

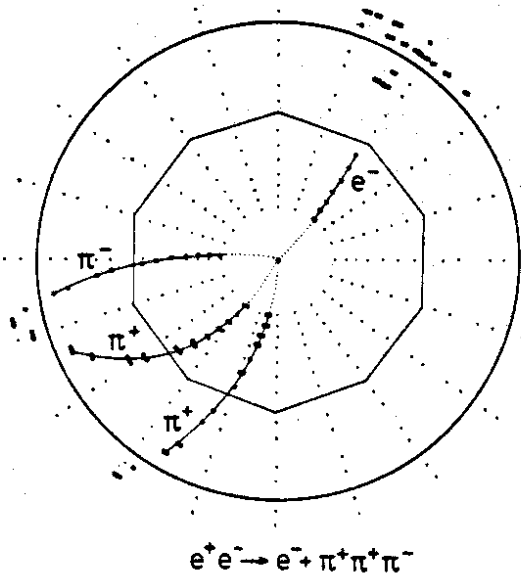


Fig. 9. Four prong event in PLUTO, view along the axis. The lead converters are indicated, the electron produces a shower.

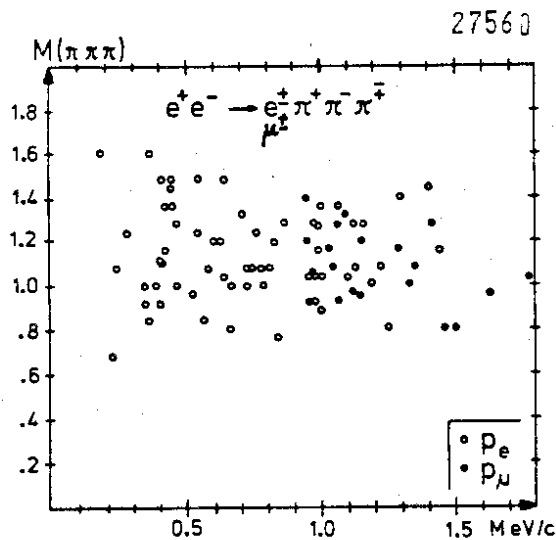


Fig. 10. Momentum distribution of leptons versus the invariant three pion mass, from the event class (5).

An event of type (5) is shown in fig. 9. The electron and the three pion system emerge from the interaction region in opposite directions as would be expected if the event is interpreted according to reaction (6).

The analysis is based on the same total data set as quoted in the last chapter. Charge balanced 4 prong events without photons are selected out of the total data, and electrons identified by an analysis of the shower pattern in the proportional chambers behind the lead converter. The method yields a misidentification of hadrons  $P_{h \rightarrow e} = 1.2\%$ , and a detection efficiency for electrons rising from 0.30 at 0.4 GeV/c to 0.65 for momenta  $p_e \geq 1.0$  GeV/c. QED-events are removed by a missing mass cut  $MM^2 \geq 0.9$  GeV<sup>2</sup>. After a final cut in momenta,  $p_e \geq 0.4$ ,  $p_\mu \geq 1.0$  GeV/c, there remain 66 events. Fig. 10 shows the event sample before the momentum cut. The invariant  $3\pi$ -mass is plotted versus momentum. The plot demonstrates that the  $3\pi$ -mass is low,  $\sim 1.1$  GeV, that the lepton spectrum is hard as

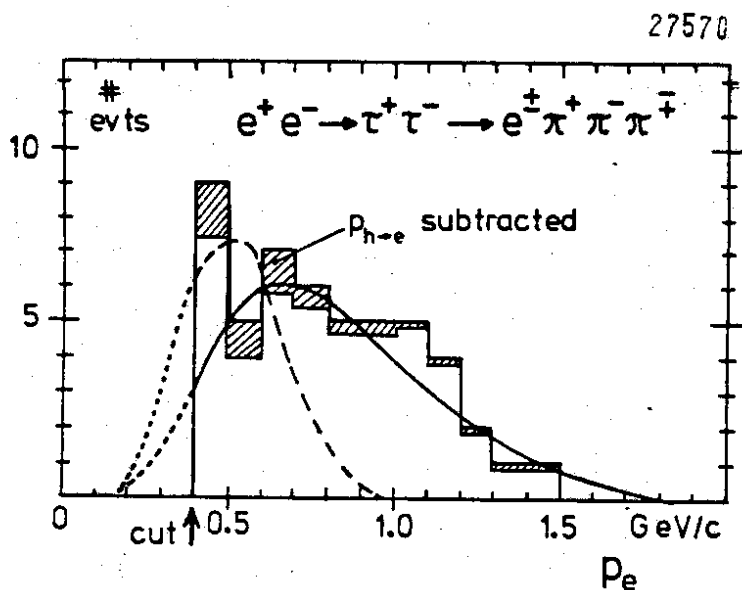


Fig. 11. Distribution of electron momenta.  
Solid line : calculation for  $\tau \rightarrow \nu e$ , normalized. Dashed line : spectrum from charm decays <sup>12</sup>, not normalized.

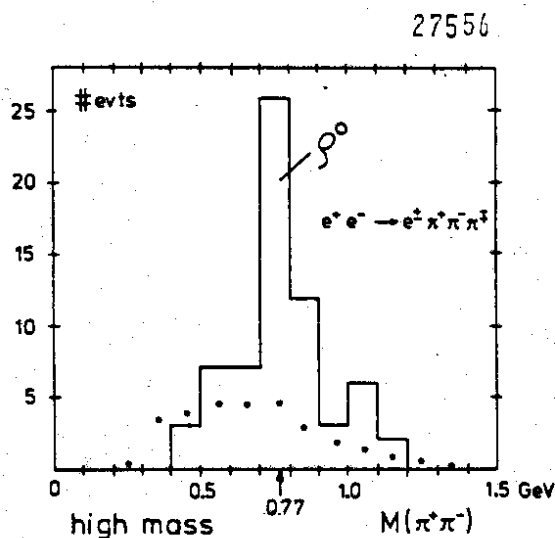


Fig. 12. Distribution of the invariant two pion mass (high solution). The black points are the experimental background, calculated from the misidentification of hadrons,  $P_{h \rightarrow e}$ .

expected from  $\tau$ -decays, and that both quantities are uncorrelated. All this is consistent with the decay of a pair of heavy particles.

Consistency with reaction (6) is further verified by the momentum distribution of electrons shown in fig. 11.

The spectrum agrees well with the calculated  $\tau$ -decay into electrons and neutrinos. An estimate of the contribution from charm decays yields at most 3 events and the spectrum is moreover soft. We therefore conclude that the three pions and the leptons are indeed coming from reaction (6).

In order to investigate the three pion system

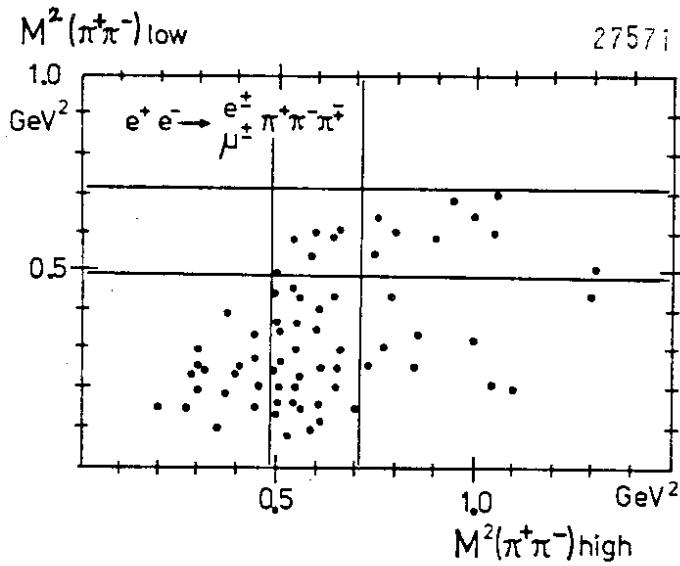


Fig. 13. Invariant mass squared,  $M(\pi^+\pi^-)^2$  in the Dalitz plot representation. The lines define the  $\rho^0$ -bands :  $0.70 \leq M(\pi^+\pi^-) \leq 0.84$  GeV.

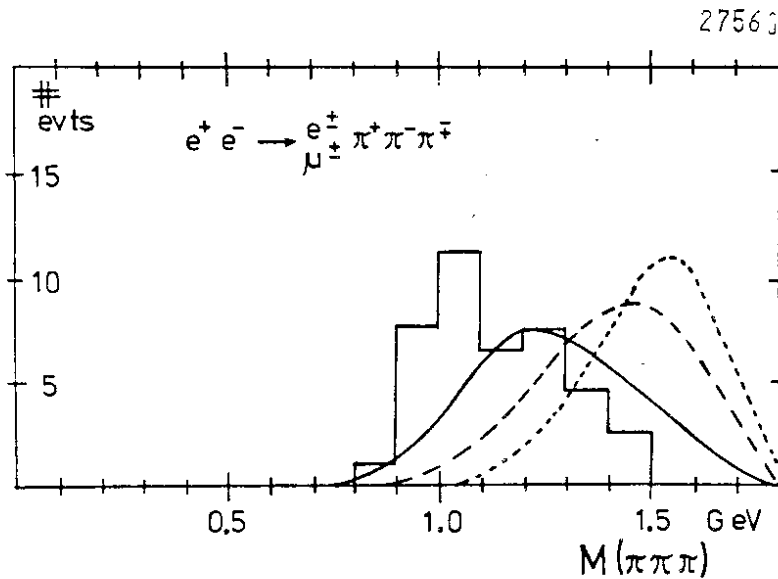


Fig. 14. Invariant  $3\pi$ -mass distribution of events within the rho-bands. Calculated  $3\pi$ -mass distributions are given for  $J^P = 1^+$ , S-wave (solid line);  $J^P = 0^-$ , P-wave (dashed); and  $J^P = 1^+$ , D-wave (dotted).

the invariant two pion mass distribution is plotted in fig. 12. A clear peak at the rho-mass is seen. It contains 33 events within the rho-band  $0.7 \leq M(\pi^+\pi^-) \leq 0.84$  GeV. The background, which is not peaked at the mass of the rho meson, contains 25 events, 6 of which lie within the rho-band.

Both, high and low solutions are shown in the Dalitz plot given in fig. 13. Out of the 66 events, a total of 42 lie within the rho-bands. In view of the 25 background events we conclude that the final state must be a pure  $\pi\rho$ -system. The branching ratio is then

calculated with the result  $BR(\tau^- \rightarrow \nu\pi^- \rho^0) = 0.052 \pm 0.012$ , consistent with the branching ratio expected on the basis of a sequential heavy lepton of  $1/2 \cdot BR(\tau^- \rightarrow \nu A_1^-) = 0.04$ <sup>13</sup>. Fig. 14 finally shows the three pion mass distribution compared with the calculated distributions of a  $\pi\rho$ -system for the three lowest angular momentum states S, P, D, which have  $J^P = 1^+, 0^-, 1^+$  respectively. Clearly, the state  $J^P = 1^+, \ell = 0$  is favoured by the data, with a resonance like peak at threshold. This result is supported by a three dimensional Dalitz plot analysis. The  $A_1$ -meson is the only known axial vector meson,  $J^P = 1^+$ , in this mass region. A preliminary mass determination yields  $M_{A_1} = 1.0$  GeV,  $\Gamma_{A_1} = 0.47$  GeV. The decay of the heavy lepton  $\tau$  into the hadronic state  $1^+$  establishes the presence of axial vector in the weak coupling.

#### THE TOTAL $e^+e^-$ HADRONIC CROSS SECTION

The total cross section for hadron production,  $\sigma_h(e^+e^- \rightarrow h)$ , measured with the PLUTO detector, is shown in fig. 15. The cross section is given in units of the cross section for muon pair production,  $R = \sigma_h/\sigma_{\mu\mu}$ , and covers the energy range from 3.6 to 5.0 GeV, with a gap between 3.7 and 4.0 GeV. Contributions to R come from the cross section for one photon annihilation,  $\sigma_{tot}$ , and the cross section for the  $\tau$ -pair production, which rises above the threshold according to  $\sigma_{\tau\tau} = \sigma_{\mu\mu} \cdot \beta \cdot (3 - \beta^2)/2$ ;  $\beta$  denotes the velocity of the  $\tau$ .  $R_\tau$  which is shown by the dashed line in figure 15, approaches one unit for  $\beta \rightarrow 1$ . It must be remembered that 85 % of the decaying  $\tau$ -pairs have hadrons in the final state; the 15 % of pure leptonic decays left have not been removed from the data because of their acollinearity. All other QED events, however, were separated by appropriate cuts.  $\sigma_{tot}$  is predicted by the triplet quark sum rule. Including QCD-corrections<sup>14)</sup> the following theoretical expression for R is then expected :

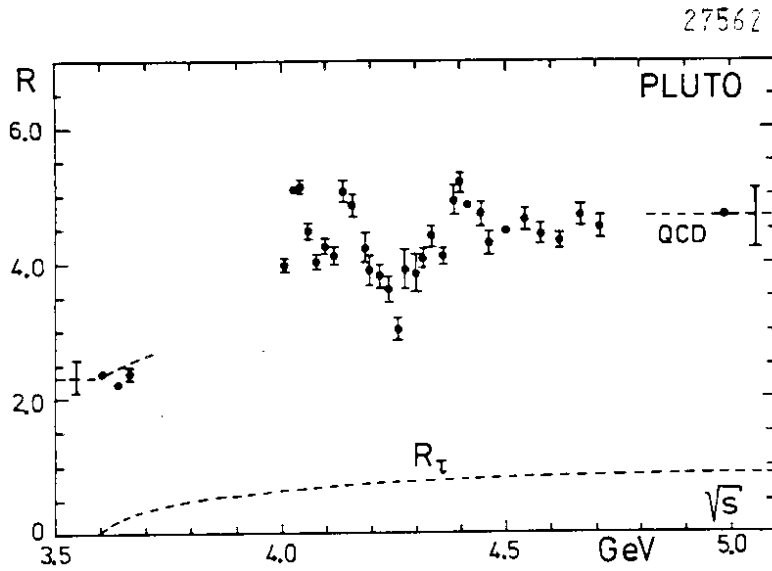


Fig. 15. Total hadronic cross section in units of  $\sigma_{\mu\mu}$  vs. center of mass energy.

$$R = \sum 3Q_i^2 (1 + \alpha(s)/\pi) + R_\tau \quad (7)$$

$Q_i$  = quark charges (u, d, s, c)

$$\alpha(s) = 12\pi / (25 \cdot \ln s/\Lambda^2)$$

The QCD-correction with the value  $\Lambda = 0.73$  GeV<sup>15)</sup>, amounts to 0.30 at  $\sqrt{s} = 3.6$  GeV, and 0.42 at  $\sqrt{s} = 5.0$  GeV. It can be seen that the data agree well with the prediction, though a definite conclusion is prohibited since the data have a systematic error of 10 % which is indicated in the figure.

The rise of the cross section seen above 4 GeV is now believed to be well understood by the new channel which opens for charm production at  $\sqrt{s} = 3.73$  GeV. If the observed peaks are interpreted as resonances (due to D, D\*, F, F\* production), a fit to the data yields the resonance parameters given in table I.



Table I Resonance parameters

M (GeV)	$\Gamma$ (keV)	$\Gamma_{ee}$ (keV)
4.035	$55 \pm 5$	$0.7 \pm 0.1$
4.146	$47 \pm 11$	$0.4 \pm 0.1$
4.400	$33 \pm 9$	$0.3 \pm 0.1$

ANGULAR DISTRIBUTION OF THE DECAY  $J/\psi \rightarrow f^0 \gamma$ 

This process has been observed in the PLUTO detector <sup>16)</sup> via the decay  $f^0 \rightarrow \pi^+ \pi^-$  at the resonance energy  $\sqrt{s} = 3.091$  GeV. The signature of the selected events is thus :

$$e^+ e^- \rightarrow J/\psi \rightarrow \pi^+ \pi^- \gamma (\pi^0) \quad (8)$$

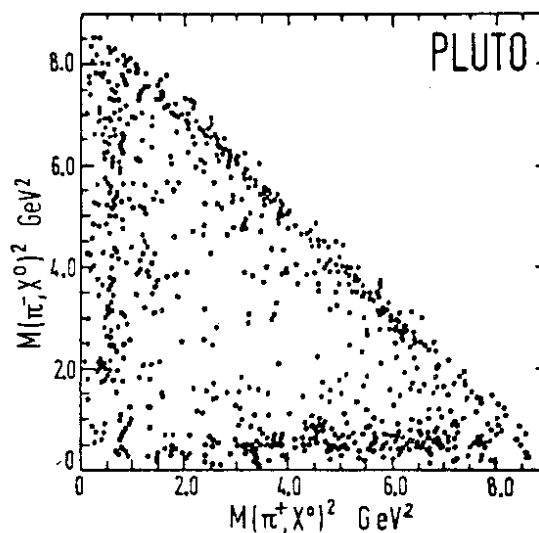
The momenta of the pions and the direction of the photon are measured. The detected photon can also be an unresolved photon pair from the decay of a neutral pion. The trigger efficiencies for  $\pi^+ \pi^- \gamma$  and  $\pi^+ \pi^- \pi^0$  are 73 % and 75 % respectively, as obtained from Monte-Carlo studies. Out of 84 000  $J/\psi$  hadronic events, 1650 survive a fit to the hypothesis (8) with  $X^2 \leq 20$ . These are further reduced to 825 events by cuts removing QED background. The distribution of these events in the Dalitz plot is shown in fig. 16, where the three rho-bands are seen to be populated. To study the neutral  $\pi^+ \pi^-$  masses we impose cuts  $0.6 \leq M(\pi^+ \pi^-) \leq 1.0$  GeV and plot the invariant mass distribution  $M(\pi^+ \pi^-)$  in fig. 17. In the figure the  $\rho^0$  - and  $f^0$ -signals are clearly visible. The solid line is a resonance fit with a polynomial background, from which the resonance parameters  $M_f = 1.23 \pm 0.04$  GeV, and  $\Gamma_f = 0.13 \pm 0.05$  GeV are obtained. Several checks assure that the signal is neither  $\rho^0$  nor  $\rho'(1250)$ .

As the  $J/\psi$  decays violate the OZI rule <sup>17)</sup>, it is of considerable interest to understand the nature of the decay mechanism.

Fig. 16.

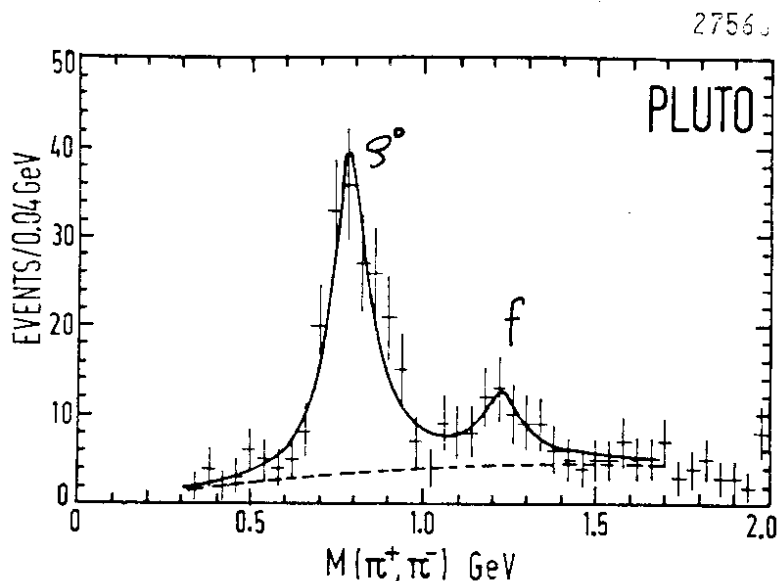
27155

Dalitz representation of  
reaction (8),  $M(\pi^- X^0)^2$  vs.  
 $M(\pi^+ X^0)^2$ ,  $X^0 = \gamma$  or  $\pi^0$



The branching ratio obtained  
for this decay is  $BR(J/\psi \rightarrow f^0 \gamma)$   
 $= (2.0 \pm 0.7) \cdot 10^{-3}$ . This rate  
can be compared with the decay  
into  $f^0 \omega$ :  $BR(J/\psi \rightarrow f^0 \omega)$   
 $= (4.0 \pm 1.4) \cdot 10^{-3}$ , ref. 18)

which has the same order of  
magnitude. This result would be incompatible with the decay diagram  
(a) of fig. 18, where we expect a ratio of order  $10^{-3}$ . However, the  
decay  $J/\psi \rightarrow f^0 \gamma$  may be dominated by a two gluon exchange, as given  
in fig. 18 (b), where photon couples directly to the  $c(\bar{c})$  quark.  
Though a rate calculation does not exist for this diagram, there  
is a calculation of the angular distribution for the  $f^0 \gamma$  system in

Fig. 17. Invariant mass distribution  $M(\pi^+ \pi^-)$

the framework of QCD<sup>19)</sup>, which offers the possibility for an experimental test<sup>20)</sup>.

2756

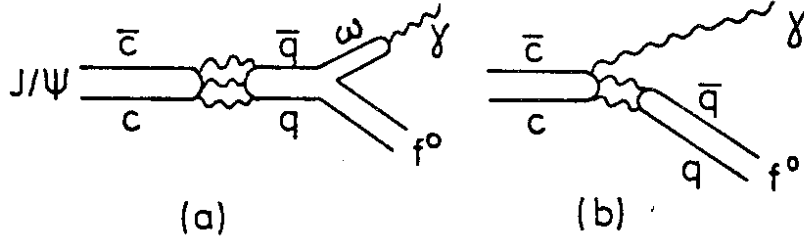


Fig. 18. Diagrams for the decay  $J/\psi \rightarrow f^0 \gamma$  with (a) three gluons, and (b) two gluons exchanged.

The angular distribution in terms of the  $f^0$ -helicity amplitudes  $A_0, A_1, A_2$ , with  $x = A_1/A_0$ , and  $y = A_2/A_0$  is given by

$$\begin{aligned}
 W_f(\delta_p, \delta_M, \phi_M) \propto & \quad (9) \\
 & 3x^2 \sin^2 \delta_p \sin^2 2\delta_M + \\
 & (1 + \cos^2 \delta_p) \left[ (3 \cos^2 \delta_M - 1)^2 + \frac{3}{2} y^2 \sin^4 \delta_M \right] - \\
 & \sqrt{3} x \sin 2\delta_p \sin 2\delta_M (3 \cos^2 \delta_M - 1 - \sqrt{\frac{3}{2}} y \sin^2 \delta_M) \cos \phi_M + \\
 & \sqrt{6} y \sin^2 \delta_p \sin^2 \delta_M (3 \cos^2 \delta_M - 1) \cos 2\phi_M,
 \end{aligned}$$

where  $\delta_p$  is the production angle between the  $f^0$ -meson and the  $e^+ -$  flight direction. The polar and azimuthal decay angles  $\delta_M$  and  $\phi_M$  are those of the  $\pi^+$ -meson measured in the helicity frame of the  $\pi^+ \pi^-$  center of mass system, where the z-axis is defined by the flight direction of the  $\pi^+ \pi^-$  - system.

The results of a fit to the data, the method of which is too elaborate to be discussed here, are given in fig. 19 by lines for constant  $\chi^2$  in the x, y-plane. The  $\chi^2$  values assigned to the contours are measured from the minimum  $\chi^2 = 26$ , marked by a cross, obtained for 25 degrees of freedom. Also shown is the QCD-prediction of  $x = 0.76, y = 0.54$ <sup>19)</sup>. The best experimental values of  $x = 0.6 \pm 0.3, y = 0.3$ <sup>+0.6</sup><sub>-1.6</sub> are in very good agreement. The same is true for the nearby values of  $x = 0.71, y = 0.41$  derived from a

tensor dominance model <sup>21)</sup>.

To check the fitting results we repeated the fit by varying the background percentage in the  $f^0$  mass band in the range of 40 - 60%, but no appreciable difference from the result given in fig. 19 were observed. A fit to only the background distributions, however, yields a rather different result, namely  $x = -1.2$ ,  $y = -0.4$  with  $\chi^2 = 77$  for 25 degrees of freedom. A final check is made by applying the method to the angular distribution of the decay  $J/\psi \rightarrow \rho^0 \pi^0$ . As fig. 17 shows

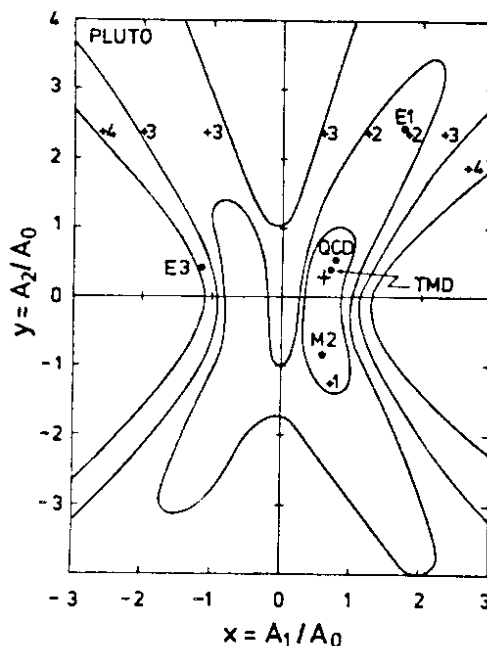
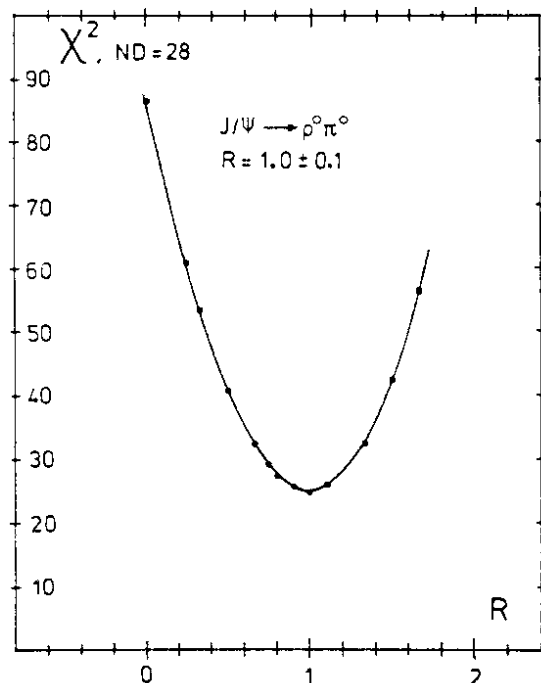


Fig. 19. Diagram of the constant  $\chi^2$  in the  $x, y$ -plane from a fit of experimental data to distribution (9).



the  $\rho^0$  is observed simultaneously with the  $f^0$ , but has to be associated with a  $\pi^0$ . The angular distribution of this process :

Fig. 20.  
Fit to the angular distribution (10) of the decay  $J/\psi \rightarrow \rho^0 \pi^0$ ,  $\chi^2$  vs.  $R$ .

$$W(\delta_P, \delta_M, \phi_M) \propto (1 + \cos^2 \delta_P) \sin^2 \delta_M + R \sin^2 \delta_P \sin^2 \delta_M \cos 2\phi_M \quad (10)$$

is described by only one independent helicity amplitude and is therefore uniquely fixed with  $R = +1$ . Our fitting procedure yields in fact  $R = 1.0 \pm 0.1$  with  $\chi^2 = 25$  for 28 degrees of freedom, see fig. 20, a result which is in excellent agreement with  $R = 1$  for the  $J^P = 1^-$  assignment to the  $J/\psi$  particle.

The decay  $J/\psi \rightarrow f^0 \gamma$  has also been observed in the DASP detector <sup>22)</sup> by requiring one pion in the outer arm, and one track with a photon in the inner, non magnetic detector. The resulting Dalitz distribution, given in fig. 21 (a), is similar to the one given in fig. 16 for the PLUTO data. Fig. 21 (b) shows the resulting invariant mass distribution, where the  $\rho^0$  and  $f^0$  mass bands are populated. The branching ratio obtained in this experiment depends

276

on the assumed angular distribution, which is unmeasurable. It is given in table II for the three radiative multipole transitions  $E_1$ ,  $M_2$ , and  $E_3$ , which are also shown for comparison in fig. 19. It can be seen that only the  $M_2$  transition lies within one standard deviation from the best value obtained by PLUTO. The branching ratio given for  $M_2$  also agrees best with the respective value obtained in the PLUTO experiment.

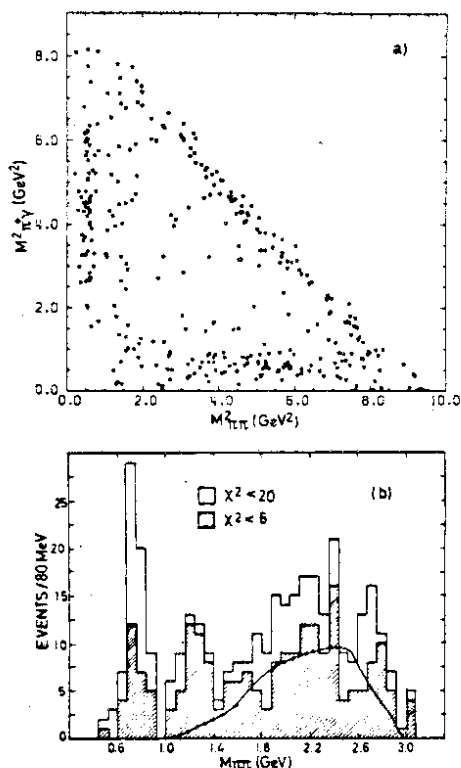


Fig. 21 (a) Dalitz plot representation of reaction (8),  
(b) Invariant mass distribution  $M(\pi^+\pi^-)$ , DASP.

Table II Branching Ratios for  $J/\psi \rightarrow f^0 \gamma$ , DASP

type of transition	branching ratio
$E_1$	$(0.9 \pm 0.3) \cdot 10^{-3}$
$M_2$	$(1.5 \pm 0.4) \cdot 10^{-3}$
$E_3$	$(1.0 \pm 0.3) \cdot 10^{-3}$

Being aware that the storage ring is an integral part of  $e^+e^-$  - physics, our thanks go to the colleagues of the DORIS operation group for their continuous and effective efforts to optimize the running conditions for experiments.

## REFERENCES

## 1. PLUTO-Collaboration

- DESY G. Alexander, L. Criegee, H.C. Dehne, K. Derikum, R. Devenish, G. Flügge, J.D. Fox, G. Franke, Ch. Gerke, E. Hackmack, P. Harms, G. Horlitz, Th. Kahl, G. Knies, H. Lehmann, R. Schmitz, R.L. Thompson, U. Timm, H. Wahl, P. Waloschek, G.G. Winter, S. Wolff, W. Zimmermann
- U. Aachen W. Wagner
- U. Hamburg V. Blobel, A. Garfinkel, B. Koppitz, E. Lohrmann, W. Lührsen
- U. Siegen A. Bäcker, J. Bürger, C. Grupen, G. Zech
- U. Wuppertal H. Meyer, M. Rössler, K. Wacker.

## 2. DASP-Collaboration

- DESY D. Cords, R. Felst, R. Fries, E. Gadermann, H. Hultschig, P. Joos, W. Kock, U. Kötz, H. Krehbil, D. Kreinick, H.L. Lynch, W.A. McNeely, G. Mikenberg, K.C. Moffeit, D. Notz, R. Rüsck, M. Schliewa, B.H. Wiik, G. Wolf
- U. Aachen R. Brandelik, W. Braunschweig, H.-U. Martyn, H.G. Sander, D. Schmitz, W. Sturm, W. Walraff
- U. Hamburg G. Grindhammer, J. Ludwig, K.H. Mess, A. Petersen, G. Poelz, J. Ringel, O. Römer, K. Sauerberg, P. Schmüser

- MPI München W.de Boer, G. Buschhorn, W. Fues, Ch.v. Gagern,  
B. Gunderson, R. Kotthaus, H. Lierl, H. Oberlack
- U. Tokyo S. Orito, T. Suda, Y. Totsuka, S. Yamada.
3. M.L. Pearl et al., Phys.Rev.Lett. 35, 1489 (1975)
  4. PLUTO-Collaboration, J. Burmester et al., Phys.Lett.68B, 297 (1977), and DESY 77/24
  5. A. Barbaro-Galtieri, Proc. 1977 Int.Symp. on Lepton and Photon Interactions at High Energ., Hamburg, Aug. 1977, page 21
  6. DASP-Collaboration, R. Brandelik et al., Phys.Lett. 73B, 109, (1978), and DESY 77/81
  7. G. Knies, Proc. 1977 Int. Symp. on Lepton and Photon Interactions at High En., Hamburg, Aug. 1977, page 93
  8. M. Murtagh, Proc. 1977 Int. Symp. on Lepton and Photon Interactions at High En., Hamburg, Aug. 1977, page 405
  9. K. Schultze, Proc. 1977 Int. Symp. on Lepton and Photon Interactions at High En., Hamburg, Aug. 1977, page 359
  10. H. Fritzsch, Phys.Lett. 67B, 451 (1977)
  11. PLUTO-Collaboration, G. Alexander et al., Phys.Lett. 73B, 99 (1978), and DESY 77/78
  12. DASP-Collaboration, R. Brandelik et al., Phys.Lett. 70B, 387, (1977), and DESY 77/41
  13. Y.S. Tsai, Phys.Rev. D4, 2821 (1971)  
M.B. Thacker, J.J. Sakurai, Phys.Lett. 36B, 103 (1971)
  14. A. DeRujula, H. Georgi, Phys.Rev. D13, 1297 (1976)  
E.C. Poggio, H.R. Quinn, S. Weinberg, Phys.Rev. D13, 1958(1976)  
R. Barbieri, R. Gatto, Phys.Lett. 66B, 181 (1977)
  15. J.H. Mulvey,  $\Lambda = 0.73 \pm 0.1$ , Report on this Conference
  16. PLUTO-Collaboration, G. Alexander et al., Phys.Lett. 72B, 493 (1978), and DESY 77/72
  17. S. Okubo, Phys.Lett. 5, 105 (1963)  
G. Zweig, CERN-Report TH 401,412 (1969)  
J. Iikuza, K. Okada, O. Shito, Proc.Theor.Phys.35, 1061 (1966)
  18. PLUTO-Collaboration, J. Burmester et al., Phys.Lett. 72B, 135 (1977), and DESY 77/50
  19. M. Krammer, DESY 78/06, Phys.Lett. to be published
  20. PLUTO-Collaboration, G. Alexander et al., Phys.Lett. to be published, and DESY 78/20
  21. W. Gampp and H. Genz, Karlsruhe University Preprint, TKP/78-4, to be published
  22. DASP-Collaboration, R. Brandelik et al., Phys.Lett.to be published, and DESY 78/01